

# Different Array Synthesis Techniques for Planar Antenna Array

Tarek Sallam<sup>1</sup> and Ahmed M. Attiya<sup>2</sup>

<sup>1</sup> Faculty of Engineering at Shoubra  
Benha University, Cairo, Egypt  
tarek.sallam@feng.bu.edu.eg

<sup>2</sup> Microwave Engineering Dept.  
Electronics Research Institute (ERI), Giza, Egypt  
attiya@eri.sci.eg

**Abstract** — In this paper, a genetic algorithm (GA) is used to synthesize and optimize the excitation weights of a planar array for satellite communications based on ITU Radio Regulations 2016. The planar array is arranged into symmetric square lattices of subarrays. Each subarray is assumed to be consisting of 4×4 isotropic, uniform-spaced, and uniform-weighted elements. The proposed arrays are assumed to be consisting of 4×4 and 16×16 subarrays. A genetic algorithm is used to optimize the weights at the subarrays. Three different cases are studied in the paper. The first case is dealing with an amplitude-only weighting synthesis of the planar array. In this case the ratios of amplitude weights of subarrays are varied continuously from 0 to 1. In the second case, a phase-only synthesis of the planar array is discussed where the phases are varied in a continuous range between  $-\pi/2$  and  $0^\circ$  while the amplitudes of all subarrays are the same. In the third case a complex weight synthesis is presented. In this case the ratios of the amplitudes are constrained between 0.7 and 1 whereas the phases are varied continuously from  $-\pi/2$  to  $0^\circ$ . Moreover, the amplitude is varied with both continuous and discrete values. A comparison between the three methods is presented to develop the optimum technique for feeding an antenna array for satellite communication systems.

**Index Terms** — Antenna array, genetic algorithm, satellite antenna.

## I. INTRODUCTION

Planar antenna arrays are good candidates for on-move earth segment of satellite communication systems [1–5]. From manufacturing point of view, it would be better to divide these planar arrays into smaller subarrays which are connected together through a common feeding network. The elements of these subarrays are usually fed with uniform distribution network. Due to the required constrains on the total radiation pattern of the complete antenna array according to the standards of the satellite

communications, uniform distribution network would not be suitable for the feeding network between the subarrays. Thus, it would be required to synthesis the appropriate distribution for these subarrays to obtain the required specifications of the radiation pattern.

However, global synthesis of antenna arrays that generate a desired radiation pattern is a highly nonlinear optimization problem. Thus, analytical methods are not applicable any more. Several classical methodologies have been proposed to obtain suitable strategies for the optimal synthesis of antenna arrays [6]. Optimization algorithms differ in the complexity of computations and convergence rate. However, from the point of view of array synthesis, the result depends on the final convergence not on the method itself. It was shown in [7–11] that the evolutionary optimization algorithms such as genetic algorithm (GA), bees algorithm, differential evolution algorithm, particle swarm optimization and colony selection algorithm are capable of performing better and more flexible solutions than the classical optimization algorithms and the conventional analytical approaches.

The GA is an excellent stochastic global optimization approach which is part of a larger field of evolutionary computations. This approach models genetics and natural selection in order to optimize a given cost function [12, 13]. Since its introduction, the GA has become a dominant numerical optimization algorithm in many disciplines. Details on implementing a GA can be found in [14], and a variety of applications to electromagnetics are reported in [15]. Some of the advantages of the GA include: (a) optimizing continuous or discrete variables, (b) avoiding calculation of derivatives, (c) handling a large number of variables, (d) suitability for parallel computing, (e) jumping out of a local minimum, (f) providing a list of optimum variables, not just a single solution, and (g) working with numerically generated data, experimental data, or analytical functions.

The GA implemented here is simple and flexible for

pattern synthesis of arbitrary arrays. This approach avoids binary coding and directly deals with real or complex weighting vectors. Using this approach, constraints on the phases and magnitudes of the complex weights are easily imposed for practical implementation of phase shifters and attenuators.

In this paper, we use the GA to synthesis the distribution network of the subarrays to obtain a complete radiation pattern which satisfies the required standards of satellite communications [14], [15]. Previous studies discussed briefly this distribution network by adjusting the amplitude of the feeding of each subarray [1-5].

On the other hand, the optimization techniques are dealing with the problem only from mathematical point of view. However, in practical application, the obtained distribution network may not be quite suitable for physical implementation. The simplest implementation of any arbitrary distribution network would be mainly composed of non-equal Wilkinson power dividers combined with lumped element resistors and transmission line sections [16]. For equal power division, the arms of the Wilkinson power divider would have equal characteristic impedance of  $\sqrt{2}Z_0$  where  $Z_0$  is the characteristic impedance of the feeding port. However, for large ratios of power divisions, the two arms of the characteristic impedance would have completely different values with very small and very large values. The large values of the characteristic impedance would correspond to very thin printed transmission line sections. On the other hand, the small values of characteristic impedance would correspond to very wide printed transmission line sections. This would introduce a quite complexity on the implementation of the non-equal power divider.

Thus, direct synthesis of the distribution network based on the amplitude only may not be quite suitable for implementation. This is the motivation in this paper to introduce the idea of using other distribution networks and compare between them. In addition to the conventional amplitude only distribution network, we introduce in this paper other three configurations, equal amplitude with non-equal phase distribution network, constrained non-equal amplitude with non-equal phase distribution network and discrete non-equal amplitude with non-equal phase distribution network. In constrained non-equal amplitude, the amplitude ratio is limited in continuous range from 0.7 to unity. However, in discrete constrained non-equal amplitude, the amplitude ratio is limited to four discrete values 0.7, 0.8, 0.9, and 1 only. This has an additional advantage in implementation where specific pre-designed power divider would be used directly as blocks in the complete distribution network. On the other hand, the non-equal phases can be simply implemented by adjusting the lengths of the transmission line sections after power division.

The present study is almost like other studies of beamforming such as null broadening beamforming [21],

constrained normalized least-mean-square (CNLMS) beamforming [22], and linearly constrained minimum variance (LCMV) beamforming [23] as well as direction of arrival (DOA) techniques such as Cramér Rao bound (CRB) approach [24] which depend mainly on the array factor. The result of the present feeding distribution function would be the starting point for full wave analysis of the complete array configuration which includes mutual coupling [25] in this case.

## II. FORMULATION OF THE PROBLEM

The complete antenna array is assumed to be composed of an array of subarrays as shown in Fig. 1. Each subarray is composed of  $N_{ex} \times N_{ey}$  elements. The complete array is composed of  $2N_{sx} \times 2N_{sy}$  subarrays. The array factor for this planar array can be presented as [17],

$$AF(\theta, \varphi) = 4 \sum_{p=1}^{N_{sy}} \sum_{q=1}^{N_{sx}} b_{pq} \sum_{m=1}^{N_{ey}} \sum_{n=1}^{N_{ex}} a_{mn} \cos(X_{qn}) \cos(Y_{pm}), \quad (1)$$

where,

$$X_{qn} = kd_x \sin \theta \cos \varphi [n - 0.5 + (q - 1)N_{ex}], \quad (2-a)$$

$$Y_{pm} = kd_y \sin \theta \sin \varphi [m - 0.5 + (p - 1)N_{ey}], \quad (2-b)$$

$a_{mn}$  represents the complex weight of radiating element in the subarray,  $b_{pq}$  represents complex weight of the subarray  $2N_{sx}$  is the number of subarrays in  $x$  direction,  $2N_{sy}$  is the number of subarrays in  $y$  direction,  $N_{ex}$  is the number of elements in the subarray in  $x$  direction,  $N_{ey}$  is the number of elements in the subarray in  $y$  direction,  $d_x$  is the spacing between the radiating elements in the  $x$  direction, and  $d_y$  is the spacing between the radiating elements in the  $y$  direction. The distribution network of the total array is weighted only at the subarray level. Thus, the amplitudes of all elements inside each subarray are unity ( $a_{mn} = 1$ , for all  $m, n$ ).

Since the planar array is symmetric about its both axes, the GA synthesizes only a quarter of the array. This quarter of the symmetric planar array is called a *unit* as shown in Fig. 2. In this case, the unit consists of  $N_{sx} \times N_{sy}$  subarrays. In all following simulations, each subarray has  $4 \times 4$  elements, and a square array is assumed. Thus,  $N_{ex} = N_{ey} = 4$  elements,  $N_{sx} = N_{sy} = N$ , and  $d_x = d_y = d$ . Moreover, it is also shown that the unit itself is symmetric about its main diagonal.

The reason for choosing a subarray of  $4 \times 4$  elements is that it would be quite complicated to design a feeding network on the same layer for a subarray of additional elements as it is shown in the proposed feeding network in [3].

The GA begins with a random set of array configurations called the *population* (rows of a matrix for linear array and matrices of a tensor in the case of planar array) consisting of variables such as element/subarray amplitude and phase. Each array configuration is evaluated by the cost function that returns a numerical value or score that characterizes how well the array

configuration performs. Array configurations with high costs are discarded, while array configurations with low costs form a mating pool. Two parents are randomly selected from the mating pool. Selection is inversely proportional to the cost. Offspring result from a combination of the parents. The offspring replace the discarded array configurations. Next, random array configurations in the population are randomly modified or mutated. Finally, the new array configurations are evaluated for their costs and the process repeats. The flowchart of the GA appears in Fig. 3.

In this paper, the array is planar, and hence each array configuration is a matrix (called *chromosome*) containing a number of columns equals the number of subarrays in  $y$  direction and a number of rows equals double the number of subarrays in  $x$  direction (the upper half for amplitude and lower half for phase). If the unit is only to be optimized, the chromosome will be  $2N \times N$  matrix.

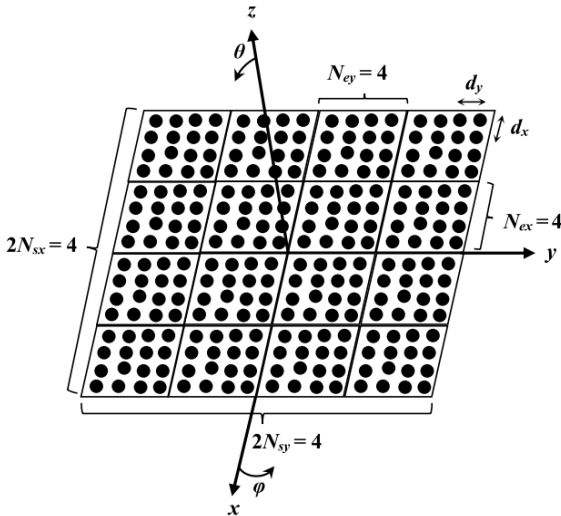


Fig. 1. Planar array with  $4 \times 4$  subarrays each having  $4 \times 4$  elements. In this case, the array is square with  $N_{ex} = N_{ey} = 4$ ,  $2N_{sx} = 2N_{sy} = 2N = 4$ , and  $d_x = d_y = d$ .

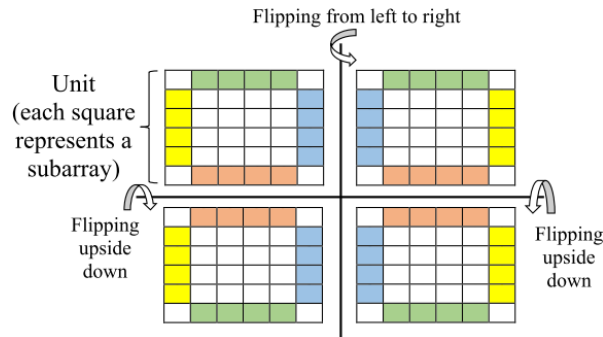


Fig. 2. A graphical representation of the whole symmetric planar array as composed from its building *unit*.

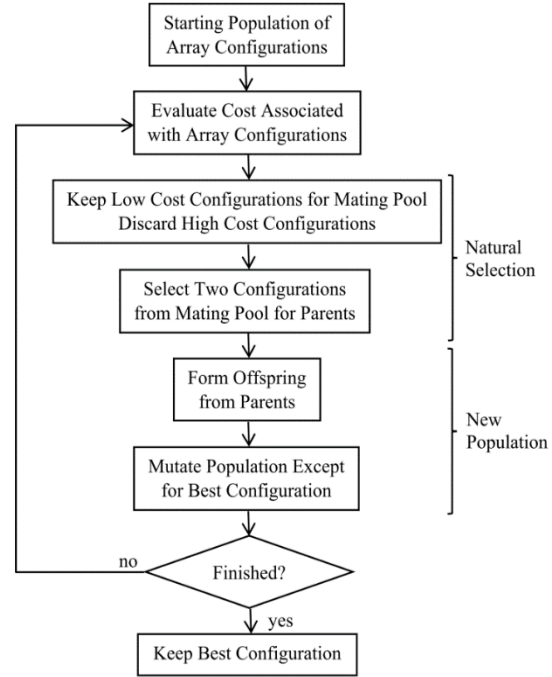


Fig. 3. Flowchart of the GA.

The cost function that is effective for the optimization of array weights for shaping the radiation pattern is defined as the error between the array factor and the required Mask and is normalized by the total number of points  $N_{tot}$  used to sample the AF and the Mask as follows:

$$\text{Cost} = \frac{1}{N_{tot}} \sum_i \frac{1 + \text{sgn}(AF(\theta_i)_{dBi} - \text{Mask}(\theta_i)_{dBi})}{2} [AF(\theta_i)_{dBi} - \text{Mask}(\theta_i)_{dBi}]. \quad (3)$$

The cost function is expressed in dBi to allow for finer improvements as the optimizer converges.

It should be noted that, only the pattern points of AF those are greater than the Mask contribute to the total score of the cost function. For this reason, this cost function is often called the “don’t exceed” square error criterion. This cost function is quite good for shaping sidelobe patterns since it does not penalize sidelobes below the mask. An optimal solution is defined as any solution which does not violate the mask, resulting in a score of zero.

It should be noted that this “don’t exceed” sidelobe threshold is a nonlinear constraint which is not generally can be handled by analytical methods such as least squares [18, 19], which require the specification of an achievable far field pattern. The “don’t exceed” sidelobe threshold case is of practical interest since usually one does not care how the sidelobes are arranged, only those are below the mask level. The main beam is excluded from the cost function. A far field pattern of  $N_{tot} = 1000$

points evenly spaced in sine space is computed for each candidate array at each cost evaluation. Here sine space refers to the sine of the far field angle  $\theta$  at a specific angle  $\varphi$ . Equally spacing pattern points in sine space rather than angle space provide a more uniform sampling of the sidelobe amplitudes. When the angle space is used, the outer sidelobes tend to be poorly represented. The lower the cost, the more fit the array distribution.

In this paper, the desired Mask function is the ITU Mask of the 2016 Edition of ITU Radio Regulations [20] which is formulated as follows:

a) In cases where the ratio between the antenna diameter (for the square planar array, which is our case, it is the array aperture length in either  $x$  or  $y$  direction) and wavelength is greater than 100, the Mask, for a given azimuth angle  $\varphi$ , is written as:

$$G(\theta) = G_{max} - 2.5 \times 10^{-3} \left(\frac{D}{\lambda}\right)^2 \text{ for } 0 \leq \theta < \theta_m, \quad (4-a)$$

$$G(\theta) = G_1 \text{ for } \theta_m \leq \theta < \theta_r, \quad (4-b)$$

$$G(\theta) = 32 - 25 \log_{10} \theta \text{ for } \theta_r \leq \theta < 48^\circ, \quad (4-c)$$

$$G(\theta) = -10 \text{ for } 48^\circ \leq \theta \leq 90^\circ, \quad (4-d)$$

where  $\theta$  is the elevation angle,  $G(\theta)$  is the antenna gain in dB,  $G_{max}$  is the main beam antenna gain in dB,  $D$  is the antenna diameter,  $\lambda$  is the wavelength, and  $G_1$  is the first sidelobe gain which is given by,

$$G_1 = 2 + 15 \log_{10} \frac{D}{\lambda}, \quad (5)$$

$\theta_m$  and  $\theta_r$  are given by:

$$\theta_m = \frac{20\lambda}{D} \sqrt{G_{max} - G_1}, \quad (6)$$

$$\theta_r = 15.85 \left(\frac{D}{\lambda}\right)^{-0.6}. \quad (7)$$

b) In cases where the ratio between the antenna diameter and wavelength is less than or equal to 100, the Mask is given by,

$$G(\theta) = G_{max} - 2.5 \times 10^{-3} \left(\frac{D}{\lambda}\right)^2 \text{ for } 0 \leq \theta < \theta_m, \quad (8-a)$$

$$G(\theta) = G_1 \text{ for } \theta_m \leq \theta < \frac{100\lambda}{D}, \quad (8-b)$$

$$G(\theta) = 52 - 10 \log_{10} \frac{D}{\lambda} - 25 \log_{10} \theta \text{ for } \frac{100\lambda}{D} \leq \theta < 48^\circ, \quad (8-c)$$

$$G(\theta) = 10 - 10 \log_{10} \frac{D}{\lambda} \text{ for } 48^\circ \leq \theta \leq 90^\circ. \quad (8-d)$$

In Fig. 4, the ITU Mask normalized with respect to  $G_{max} = 31$  dBi of an array of  $4 \times 4$  subarrays ( $16 \times 16$  isotropic elements) with inter-element spacing  $d$  of  $0.65\lambda$  is plotted against its original uniform (non-optimized) AF at  $\varphi = 0^\circ$ . Note that the Mask is symmetric about  $\theta = 0^\circ$ . The ultimate cost function value (UCFV) in this case is 12.96 dBi. Figure 5 shows the original uniform AF of  $16 \times 16$ -subarray array ( $64 \times 64$  elements) also plotted against its normalized ITU Mask, but this time with  $d = 0.7\lambda$  and  $G_{max} = 35$  dBi. The UCFV now becomes 8.69 dBi.

In the following section, different schemes of weighting distribution functions are obtained by using genetic algorithm to satisfy the conditions of this Mask.

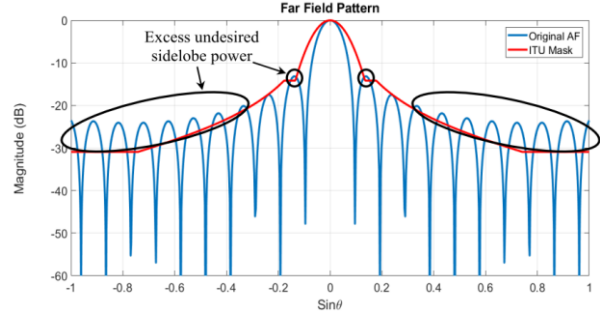


Fig. 4. The normalized ITU Mask of an array of  $4 \times 4$  subarrays with  $d = 0.65\lambda$  and  $G_{max} = 31$  dBi plotted against its original uniform AF at  $\varphi = 0^\circ$ .

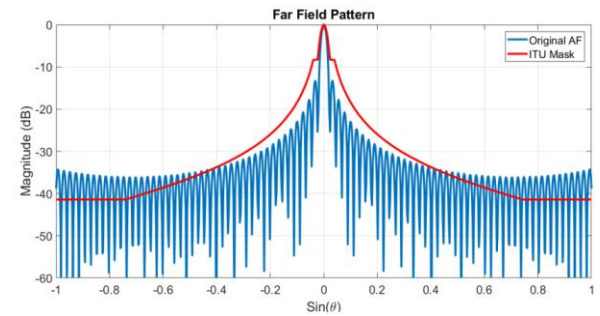


Fig. 5. The normalized ITU Mask of an array of  $16 \times 16$  subarrays with  $d = 0.7\lambda$  and  $G_{max} = 35$  dBi plotted against its original uniform AF at  $\varphi = 0^\circ$ .

### III. RESULTS AND DISCUSSIONS

The subarray excitation is represented as a complex valued weight  $b_{pq}$  with amplitude and phase. The proportions of amplitude, phase or both among subarrays can be altered to achieve the desired ITU response. In general, varying the amplitude and phase excitation offer more flexibility in the shaping of sidelobe power than aperiodic spacings between elements does. The strategy here is to implement the GA to design planar phased array antennas by controlling the weighted excitation applied to each subarray in the array while maintaining periodic element (or subarray) spacings. The GA is employed to perform amplitude-only, phase-only, and complex (both amplitude and phase) synthesis. In all simulations, an initial population of 10 random candidate array distributions is generated and evolved for 1,000 iterations (10,000 cost function evaluations).

#### A. Amplitude-only synthesis

First, we begin with the amplitude-only tapering of the planar array of  $4 \times 4$  subarrays (the same array of Fig. 4). The subarray amplitude weights are allowed to vary continuously between 0 and 1 while all phases are kept at  $0^\circ$ . In this case, the unit is  $2 \times 2$  subarrays ( $N = 2$ ), thus

the total number of optimization variables is  $N^2 = 4$ . The array has a periodic element spacing  $d = 0.65\lambda$  and a maximum gain  $G_{max} = 31$  dBi. The optimized AF of this array at  $\varphi = 0^\circ$  is shown in the bottom of Fig. 6.

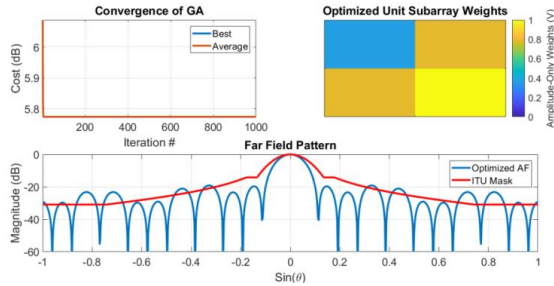


Fig. 6. The same array of Fig. 4 with amplitude-only synthesis of the array.

The convergence of the GA as a function of iteration is shown in the top left of the figure indicating that the UCFV is 5.77 dBi. The GA gives the optimized unit subarray amplitude weight values as shown in the top right of the figure. In comparison with the result in [1], the GA can give the same optimized unit subarray amplitude weight values of  $\begin{pmatrix} 0.6 & 0.8 \\ 0.8 & 1 \end{pmatrix}$ , but with a higher UCFV of 8.72 dBi. Thus, the result of the proposed approach, represented in Fig. 6, is better than that of [1].

Figure 7 shows the amplitude-only synthesis of the  $16 \times 16$ -subarray array of Fig. 5. The unit in this case is  $8 \times 8$  subarrays with  $N = 8$ . Thus, there are  $N^2 = 64$  total variables (subarray amplitude weights) for optimization. The amplitudes are varied continuously between 0 and 1. From the convergence curve of GA in Fig. 7, the UCFV is found to be 0.61 dBi.

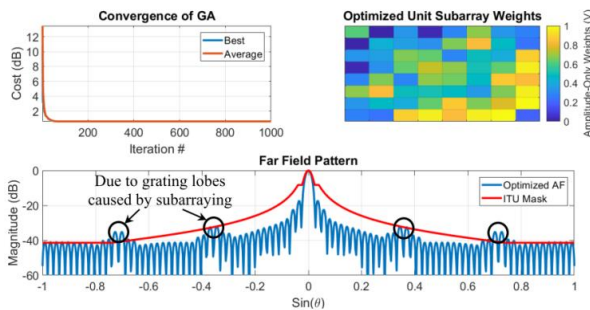


Fig. 7. The same array of Fig. 5 with amplitude-only synthesis of the array.

## B. Phase-only synthesis

Amplitude-only synthesis of the weights of subarrays is simple linear optimization with fast convergence. However, the amplitude-only synthesis has a wide variation range in amplitude between 0 and 1. This wide range causes difficulties in the practical implementation of the feeding network. This is the motivation to study the

possibility of synthesizing the array far field radiation pattern by varying the phases of the subarrays. This process of phase tapering is known as phase-only array synthesis. One of the main advantages of phase-tapered arrays is the relatively simple feed network that is required compared to amplitude tapered arrays.

The phase-only synthesis problem generally requires the application of nonlinear (the unknown phases appear in the complex exponent and are not easily found) optimization techniques for its solution.

Figure 8 shows the phase-only synthesis of the  $4 \times 4$ -subarray with the same parameters ( $N$ ,  $d$ , and  $G_{max}$ ) as of the amplitude-only weighted array in Fig. 6. With unity amplitude weighting, the unit has a total of  $N^2 = 4$  subarray phase weights as the optimization variables with their values are allowed to vary continuously from  $-\pi/2$  to  $0^\circ$ . It is clearly visible from Fig. 8 that the phase tapers have a modest ability to lower sidelobes and tend to be less efficient than amplitude tapers (the cost function cannot be fully satisfied and reaches to 9.21 dBi as an ultimate value).

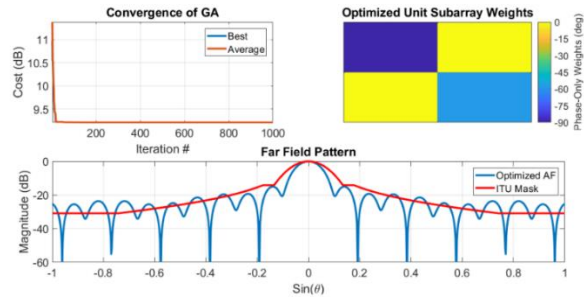


Fig. 8. As in Fig. 6, but with phase-only synthesis of the array.

Figure 9 shows the phase-only synthesis of the  $16 \times 16$ -subarray array with the same parameters as of the amplitude-only weighted array in Fig. 7. The unit has a total of  $N^2 = 64$  subarray phase weights as the optimization variables with their values are also allowed to vary continuously from  $-\pi/2$  to  $0^\circ$ . Again, as seen from Fig. 9, the cost function cannot be fully satisfied with the UCFV is just 1.91 dBi.

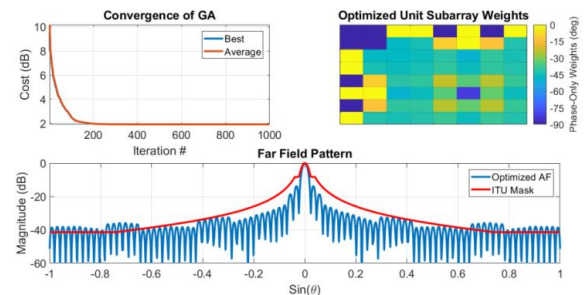


Fig. 9. As in Fig. 7, but with phase-only synthesis of the array.

### C. Complex synthesis

In order to combine the advantage of amplitude-only synthesis from the point of view of easy linear optimization and fast convergence with the advantage of phase-only synthesis from the point of view of practical implementation, a complex (amplitude and phase) synthesis of the previous arrays is presented in this Section. However, in this case the amplitude is constrained between 0.7 and 1 to obtain a simpler feeding network. Two scenarios for varying the amplitudes are discussed, continuous variation, and discrete variation with four fixed values (0.7, 0.8, 0.9, and 1). The second scenario is more appropriate for implementation where pre-designed power divider would be used as blocks in the feeding network. In both cases, the phase is varied continuously from  $-\pi/2$  to  $0^\circ$ . In this case, the total number of optimization variables (both subarray amplitude and phase weights of the unit) is  $2N^2$ .

Figure 10 shows the complex synthesis of the  $4 \times 4$  array when the amplitude is varied in a continuous way. It can be noted that the cost function reaches 6.04 dBi as an ultimate value which is above the value of the amplitude-only synthesis by only 0.27 dBi and much better than the value of the phase-only synthesis. Figure 11 shows the complex synthesis of the same array but with the discrete variation of amplitude leading to the same optimized complex weights and also the same UCFV as of the continuous variation case but with a little different convergence.

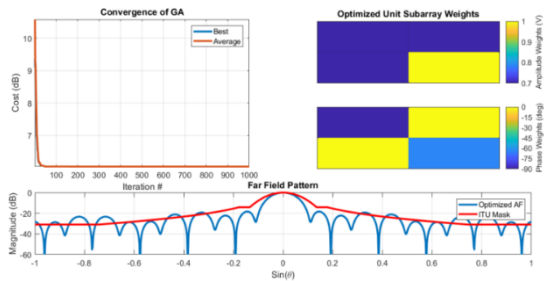


Fig. 10. As in Fig. 6, but with complex synthesis of the array. The amplitude is varied continuously in the range from 0.7 to 1.

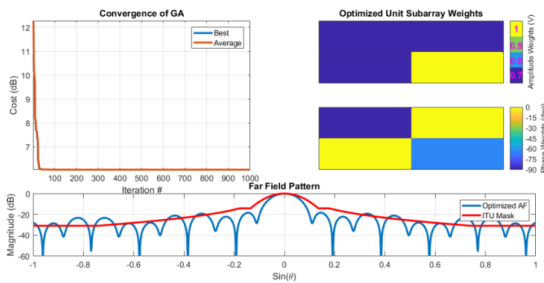


Fig. 11. As in Fig. 6, but with complex synthesis of the array. The amplitude is varied in discrete values 0.7, 0.8, 0.9 and 1.

Figure 12 shows the complex synthesis of the  $16 \times 16$  array with the continuous variation of amplitude. The cost function reaches 0.65 dBi as an ultimate value which is nearly the same value of the amplitude-only synthesis and is also better than the value of the phase-only synthesis. Figure 13 shows the complex synthesis with the discrete variation of amplitude having a simpler feed network but at the price of a higher UCFV, it is now 0.90 dBi, than that of the continuous variation.

Of all the scenarios addressed in this work, this particular scenario was the most difficult to optimize and require more iterations to converge than the previous two scenarios and this can be clearly seen from the convergence curves of Figs. 10-13. Also, note that in all previous results, the unit is symmetric about its main diagonal. Table 1 summarizes the UCFV's of the two arrays for all types of synthesis discussed as well as the uniform case.

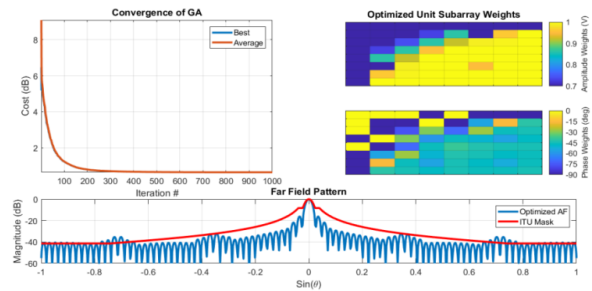


Fig. 12. As in Fig. 7, but with the complex synthesis of the array with continuous amplitude variation from 0.7 to 1.

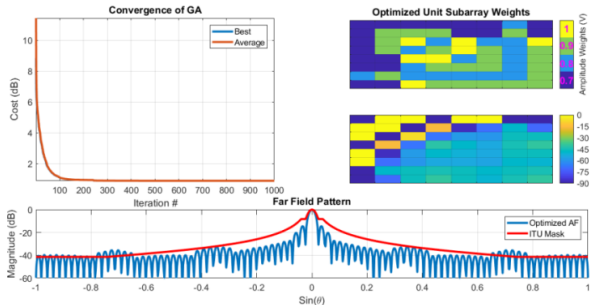


Fig. 13. As in Fig. 7, but with complex synthesis of the array. The amplitude is varied in discrete values 0.7, 0.8, 0.9, and 1.

Table 1: The summary of the UCFV's (in dBi) of the two arrays

Type of Synthesis	$4 \times 4$	$16 \times 16$
Uniform	12.96	8.69
Amplitude-only	5.77	0.61
Phase-only	9.21	1.91
Complex continuous	6.04	0.65
Complex discrete	6.04	0.90

#### IV. CONCLUSION

In this paper, four synthesis techniques are presented to optimize the radiation pattern of an antenna array to satisfy the requirements of ITU Mask for satellite communications. The techniques are, amplitude only distribution, phase only distribution, complex distribution with constrained amplitudes and complex amplitudes with discrete amplitudes. Based on the obtained results, the last two techniques are found to be the suitable ones for obtaining a good performance and practical implementation schemes.

#### ACKNOWLEDGMENT

This work was supported by Information Technology Industry Development Agency, ITIDA, Egypt, Information Technology Academia Collaboration (ITAC) program, Project No. PRP2018.R24.1.

#### REFERENCES

- [1] A. García-Aguilar, J. M. Inclán-Alonso, L. Vigil-Herrero, J. M. Fernández-González, and M. Sierra-Pérez, "Printed antenna for satellite communications," *IEEE International Symposium on Phased Array Systems and Technology (ARRAY)*, pp. 529-535, 2010.
- [2] Y.-B. Jung, S.-Y. Eom, and S.-I. Jeon, "Experimental design of mobile satellite antenna system for commercial use," *IEEE Transactions on Consumer Electronics*, vol. 56, 2010.
- [3] A. García-Aguilar, J. M. Inclán-Alonso, L. Vigil-Herrero, J. M. Fernández-González, and M. Sierra-Pérez, "Low-profile dual circularly polarized antenna array for satellite communications in the X band," *IEEE Transactions on Antennas and Propagation*, vol. 60, pp. 2276-2284, 2012.
- [4] H. T. Zhang, W. Wang, M. P. Jin, and X. P. Lu, "A dual-polarized array antenna for on-the-move applications in Ku-band," *IEEE-APS Topical Conference on Antennas and Propagation in Wireless Communications (APWC)*, pp. 5-8, 2016.
- [5] J. M. Inclán-Alonso, A. García-Aguilar, L. Vigil-Herrero, J. M. Fernández-González, J. SanMartín-Jara, and M. Sierra-Pérez, "Portable low profile antenna at X-band," *Proceedings of the 5th European Conference on Antennas and Propagation (EUCAP)*, pp. 1923-1927, 2011.
- [6] T. S. Angell and A. Kirsch, *Optimization Methods in Electromagnetic Radiation*. Springer Science & Business Media, 2004.
- [7] G. K. Mahanti, A. Chakrabarty, and S. Das, "Phase-only and amplitude-phase synthesis of dual-pattern linear antenna arrays using floating-point genetic algorithms," *Progress In Electromagnetics Research*, vol. 68, pp. 247-259, 2007.
- [8] K. Guney and M. Onay, "Amplitude-only pattern nulling of linear antenna arrays with the use of bees algorithm," *Progress In Electromagnetics Research*, vol. 70, pp. 21-36, 2007.
- [9] S. Yang, Y. B. Gan, and A. Qing, "Antenna-array pattern nulling using a differential evolution algorithm," *Int. J. Microwave RF Computer-aided Engineering*, vol. 14, pp. 57-63, 2004.
- [10] M. M. Khodier and C. G. Christodoulou, "Linear array geometry synthesis with minimum sidelobe level and null control using particle swarm optimization," *IEEE Trans. Antennas Propagat.*, vol. 53, pp. 2674-2679, 2005.
- [11] A. Akdagli and K. Guney, "A clonal selection algorithm for null synthesizing of linear antenna arrays by amplitude control," *Journal of Electromagnetic Waves and Applications*, vol. 20, pp. 1007-1020, 2006.
- [12] J. H. Holland, "Genetic algorithms," *Scientific American*, pp. 66-72, July 1992.
- [13] D. E. Goldberg, *Genetic Algorithms in Search, Optimization, and Machine Learning*. Reading, MA: Addison-Wesley, 1989.
- [14] R. L. Haupt and S. E. Haupt, *Practical Genetic Algorithms*. 2nd edition, New York: John Wiley & Sons, 2004.
- [15] R. L. Haupt and D. Werner, *Genetic Algorithms in Electromagnetics*. New York: John Wiley & Sons, 2007.
- [16] D. M. Pozar, *Microwave Engineering*. 4th edition, John Wiley & Sons, 2012.
- [17] R. Haupt, "Optimization of subarray amplitude tapers," *IEEE APS Symp.*, pp. 1830-1833, June 1995.
- [18] H. Hirasawa and B. J. Strait, "On a method for array design by matrix inversion," *IEEE Trans. Antennas Propagat.*, vol. 19, pp. 446-447, May 1971.
- [19] B. D. Carlson and D. Willner, "Antenna pattern synthesis using weighted least squares," *IEE Proc.-H*, vol. 139, no. 1, pp. 11-16, Feb. 1992.
- [20] "Methods for the determination of the coordination area around an earth station in frequency bands between 100 MHz and 105 GHz," *2016 Edition of ITU Radio Regulations*, vol. 2, appendix 7, 2016.
- [21] W. Li, Y. Zhao, Q. Ye, and B. Yang, "Adaptive antenna null broadening beamforming against array calibration error based on adaptive variable diagonal loading," *International Journal of Antennas and Propagation*, vol. 2017, Article ID 3265236, 2017.
- [22] J. F. de Andrade, Jr., M. L. R. de Campos, and J. A. Apolinário, Jr., "L1-constrained normalized LMS algorithms for adaptive beamforming," *IEEE Trans. Signal Process.*, vol. 63, no. 24, pp. 6524-6539, Dec. 2015.
- [23] J. Xu, G. Liao, S. Zhu, and L. Huang, "Response vector constrained robust LCMV beamforming

based on semidefinite programming,” *IEEE Trans. Signal Process.*, vol. 63, no. 21, pp. 5720-5732, Nov. 2015.

- [24] J. P. Delmas, M. N. El Korso, H. Gazzah, and M. Castella, “CRB analysis of planar antenna arrays for optimizing near-field source localization,” *Signal Process.*, vol. 127, pp. 117-134, 2016.
- [25] K. Yu, Y. Li, and X. Liu, “Mutual coupling reduction of a MIMO antenna array using 3-D novel meta-material structures,” *Applied Computational Electromagnetics Society Journal*, vol. 33, no. 7, pp.758-763, 2018.



**Tarek Sallam** was born in Cairo, Egypt, in 1982. He received the B.S. degree in Electronics and Telecommunications Engineering and the M.S. degree in Engineering Mathematics from Benha University, Cairo, Egypt, in 2004 and 2011, respectively, and the Ph.D. degree in Electronics and

Communications Engineering from Egypt-Japan University of Science and Technology (E-JUST), Alexandria, Egypt, in 2015. He was a Researcher Assistant with the High Frequency Lab, National Institute of Standards (NIS), Giza, Egypt from 2005 to 2006. In 2006, he joined the Department of Engineering Mathematics and Physics,

Faculty of Engineering at Shoubra, Benha University, where he is currently an Assistant Professor. He was a Visiting Researcher with the Electromagnetic Compatibility Lab, Department of Information and Communications Technology, Graduate School of Engineering, Osaka University, Osaka, Japan, from August 2014 to May 2015. His research interests include evolutionary optimization, artificial neural networks, phased array antennas with array signal processing and adaptive beamforming, and phased array radar with weather radar as a special case. His recent research has been on non-periodic and random antenna arrays.



**Ahmed M. Attiya** M.Sc. and Ph.D. Electronics and Electrical Communications, Faculty of Engineering, Cairo University at 1996 and 2001 respectively. He joined Electronics Research Institute as a Researcher Assistant in 1991. In the period from 2002 to 2004 he was a Postdoc in Bradley Department of Electrical and Computer Engineering at Virginia Tech. In the period from 2004 to 2005 he was a Visiting Scholar in Electrical Engineering Dept. in University of Mississippi. In the period from 2008 to 2012 he was a Visiting Teaching Member in King Saud University. He is currently Full Professor and the Head of Microwave Engineering Dept. in Electronics Research Institute. He is also the Founder of Nanotechnology Lab. in Electronics Research Institute.